Sex-differences in the genetic architecture of individual recombination rates in wild house sparrows (*Passer domesticus*).

John B. McAuley[1,*], Bertrand Servin[2], Lucy Peters[1,2], Ingerid J. Hagen[3,4], Alina K. Niskanen[3,5], Thor Harald Ringsby[3], Arild Husby[3,6], Henrik Jensen[3], Susan E. Johnston[1,*]

[1] Institute of Ecology and Evolution, School of Biology, University of Edinburgh, Edinburgh, EH9 3FL, United Kingdom.

[2] GenPhySE, Université de Toulouse, INRAE, ENVT, 31326 Castanet Tolosan, France.

[3] Centre for Biodiversity Dynamics, Department of Biology, Norwegian University of Science and Technology, 7491 Trondheim, Norway.

[4] Norwegian Institute for Nature Research, Høgskoleringen 9, 7034 Trondheim, Norway

[5] Ecology and Genetics Research Unit, University of Oulu, 90014 Oulu, Finland.

[6] Department of Ecology and Genetics, Uppsala University, 75236 Uppsala, Sweden.

* Corresponding authors: J.B.McAuley@sms.ed.ac.uk and Susan.Johnston@ed.ac.uk

Abstract

Meiotic recombination is a fundamental feature of sex and an important driver of diversity in eukaryotic genomes. It ensures proper chromosome disjunction, increases responses to selection, and prevents mutation accumulation; however, it is also mutagenic and can break up favourable haplotypes built up by selection. This cost/benefit dynamic is likely to vary depending on mechanistic and evolutionary contexts, and indeed, recombination rates show huge variation within and between chromosomes, individuals, sexes, populations, and species. Identifying the genetic architecture of recombination rates is a key step in understanding the causes and consequences of this variation. Here, we investigate broad-scale recombination landscapes and individual crossover (CO) rates in a wild population of house sparrows (*Passer domesticus*). We integrated pedigree data with ~61K SNPs to identify autosomal CO counts (ACC) and intra-chromosomal allelic shuffling ($\bar{r}_{intra}$) in 2,802 gametes. Females had longer autosomal genetic maps (2558.1cM vs 2069.6cM), 1.37 times higher ACC, and 1.46 times higher $\bar{r}_{intra}$ than males. ACC was heritable in females (h^2 = 0.23) but not in males, indicating genetic independence of male and female crossover rates. Conversely, $\bar{r}_{intra}$ was heritable in males (h^2 = 0.07), but not in females. Neither measure was associated with age or common environment effects. Genome-wide association studies of female ACC and male $\bar{r}_{intra}$ found no significant loci, but ~2% of SNPs had non-zero effects on female ACC. Our results suggest that recombination rates in house sparrows are polygenic and driven by many small-effect loci that may act in *cis* (e.g. local recombination hotspots and modifiers) or *trans* (global recombination modifiers). This work shows that recombination rates have evolutionary potential in wild birds, and provides a foundation for understanding associations between recombination rates, genome architecture, and individual fitness.

Introduction

Meiotic recombination is an essential process in sexual reproduction and has a key role in generating diversity in eukaryotic genomes (Coop and Przeworski 2007). Recombination can be beneficial; it ensures proper segregation of chromosomes, prevents the accumulation of deleterious alleles, and increases the speed at which populations can respond to selection by generating novel allelic combinations (Hill and Robertson 1966; Felsenstein 1974; Otto and Lenormand 2002). On the other hand, recombination can increase the risk of mutations and chromosomal rearrangements at crossover sites, and can break down favourable allele combinations previously built up by selection (Charlesworth and Barton 1996; Halldorsson *et al.* 2019). Trade-offs between the costs and benefits of recombination were thought to impose tight constraints on the number of crossovers per chromosome arm (Pardo-Manuel de Villena and Sapienza 2001); however, recent studies have shown extensive variation in recombination rate both within and between chromosomes, individuals, populations, sexes, and species (Myers *et al.* 2005; Coop and Przeworski 2007; Stapley *et al.* 2017). The cost-benefit dynamic of recombination rate is likely to vary depending on evolutionary context; if rates are heritable (i.e. there is underlying additive genetic variation), then they have the potential to respond to selection. Therefore, understanding the genetic basis of recombination rates is a critical first step in determining if and how they are contributing to adaptation, and how they themselves are evolving.

A large body of theory on the evolution of recombination rate exists (Felsenstein 1974; Otto and Lenormand 2002; Hartfield and Keightley 2012; Ortiz-Barrientos *et al.* 2016), yet studies investigating the adaptive potential and value of recombination rate remain limited (Ritz *et al.* 2017; Stapley *et al.* 2017). However, with the advent of tractable genomic technologies, we can begin to parse apart how and why recombination rates vary within and between individuals. This makes it possible to not only identify the heritability of recombination rates, but also its genetic architecture – that is, the effect sizes and distributions of the gene variants that contribute to heritable variation. Recent studies of individual variation and genetic architecture of recombination rates are predominantly in mammals, including model species such as humans and mice (Reynolds *et al.* 2013; Kong *et al.* 2014); livestock such as cattle, sheep and pigs (Kadri *et al.* 2016; Petit *et al.* 2017; Johnsson *et al.* 2021; Brekke *et al.* 2022b), and wild mammals from long-term studies, such as Soay sheep and red deer (Johnston *et al.* 2016, 2018). These studies integrate large pedigrees and high-density single nucleotide polymorphism (SNP) information to infer meiotic crossover positions and counts in thousands of gametes transmitted from parents to offspring. Then, heritabilities and underlying gene variants affecting recombination rates are identified using generalised linear mixed “animal models” and genome-wide association studies (GWAS). These studies have not only been instrumental in demonstrating that individual crossover counts can be heritable and associated with particular gene variants, but that they also have conserved genetic architecture between mammalian species. These studies also demonstrate that recombination rates and

their underlying genetic architectures can differ between the sexes, a phenomenon known as heterochiasmy (Lenormand and Dutheil 2005).

However, the patterns observed in these populations may not be generalisable to other (non-mammal) systems, as they have several unusual features. Humans have particularly long periods of meiotic arrest in females, where chiasma formed in the foetal ovary are not completed until adulthood (MacLennan *et al.* 2015), and higher crossover rates are associated with having more offspring, particularly in later life (Kong *et al.* 2004). Mice have variation in centromeric Robertsonian fusions that can affect crossover distributions (Capilla *et al.* 2014; Garagna *et al.* 2014); and livestock are often subject to strong and sustained directional selection, which theoretically imposes indirect selection for increased recombination in these effectively small populations (Otto and Barton 2001; Ross-Ibarra 2004; but see Muñoz-Fuentes *et al.* 2015). Furthermore, in most mammals, the positioning of recombination hotspots is determined by *PRDM9*, a gene coding for a zinc finger protein that binds to particular sequence motifs in the genome (Baudat *et al.* 2010). As crossover repair is mutagenic, this can erode the recognised motifs and reduce the number of binding sites, leading to rapid evolution of *PRDM9* alleles and a corresponding rapid turnover of hotspots (Myers *et al.* 2010; Grey *et al.* 2018). Indeed, *PRDM9* is one of the fastest evolving genes in mammals and some reptiles and fish, where it is likely to have a similar effect on hotspots, but it has also been lost from clades such as birds and amphibians, where recombination hotspots are stable (Singhal *et al.* 2015; Baker *et al.* 2017). Therefore, further research in both wild and non-mammalian systems is required to determine not only the genetic architecture of recombination, but also how it is affected by other intrinsic and extrinsic variation, particularly in natural environments.

Avian systems present a unique opportunity for further developing our understanding of the genetic basis of recombination rate variation in the wild. Birds lack *PRDM9* and have highly conserved, stable recombination hotspots that are enriched at transcription start sites (TSS) and gene promotor regions (Singhal *et al.* 2015). This may be because increased chromatin accessibility for gene transcription allows the protein SPO11 to accumulate in open chromatin regions and form double strand breaks required for crossover formation (Pan *et al.* 2011). Furthermore, a recent study in layer chickens suggested that recombination rates can be heritable ($h^2 \approx 0.17$), with underlying quantitative trait loci (Weng *et al.* 2019). A number of non-migratory, wild bird populations have been subject to long-term, individual based studies of their ecology and evolution. As genomic and pedigree data for these populations continue to proliferate, this presents a timely opportunity to investigate recombination rates in wild, non-mammal systems, and ultimately, the relationships between recombination rates, their genetic architectures, and individual fitness components (i.e. reproductive success and offspring viability).

Here, we examine variation in individual recombination rate and its genetic architecture in a wild meta-population of house sparrows (*Passer domesticus*) in Helgeland, Norway. House sparrows are small

passerine birds native to Eurasia, and are now distributed across most human-habited areas of the world. They are human commensals, often found in cities and farmland, and their ubiquity makes them a model system for ecology, evolution and adaptation (Anderson 2006). House sparrows in the Helgeland archipelago have low dispersal from their natal island, allowing for detailed data on survival and reproduction to be collected since 1993 (Jensen *et al.* 2004; Pärn *et al.* 2012). This population has extensive genomic resources, including a reference genome (Elgvin *et al.* 2017), a 6.5K SNP linkage map (Hagen *et al.* 2020), high-density SNP array (Lundregan *et al.* 2018) and a genetic pedigree (Niskanen *et al.* 2020), creating a timely opportunity to investigate recombination rate variation in a natural bird system. In this study, we characterise individual recombination rates using SNP and pedigree data to determine: (a) how recombination varies at the broad scale across chromosomes; (b) the influence of intrinsic (individual) and extrinsic (environment) effects on recombination rates; (c) the heritability of individual recombination rates; and (d) the genetic architecture of recombination rate variation.

Material and Methods

Study system.

All data was collected from the meta-population of house sparrows inhabiting an 18-island archipelago off the Helgeland coast in Northern Norway (66º39'N, 12º30'E), which has been subject to a long-term study since 1993 (Jensen *et al.* 2004). Birds are routinely captured from the beginning of May to the middle of August using mist nets, and small (25 µl) blood samples are collected from the brachial vein. Metapopulation-level pedigree construction for the Helgeland archipelago was previously done using 605 SNP markers in the R package Sequoia v2.3.1 (Huisman 2017; Niskanen *et al.* 2020). Individual hatch year was determined as either (a) the first year recorded for nestlings or fledged juveniles captured in the summer and autumn, or (b) the year prior to first year recorded for birds ringed as adults; hatch island is also recorded alongside hatch year (Saatoglu *et al.* 2021; Ranke *et al.* 2021).

SNP datasets.

SNP genotyping and Quality Control: All SNPs used in our analysis were taken from the custom house sparrow Affymetrix 200k SNP array based on the resequencing of 33 individual house sparrows (Lundregan *et al.* 2018). SNPs on the array are distributed across 29 autosomes in the house sparrow genome (chromosome 16 was excluded as sequences on this chromosome are difficult to assemble due to containing the highly repetitive major histocompatibility complex). A total of 3,116 adults were genotyped on this array. For GWAS analysis, the original 200k SNP array was subject to quality control in PLINK v1.90 (Purcell *et al.* 2007). Mendelian errors were masked using the flag *--set-me-missing*, and loci with a minor allele frequency of < 0.05 were discarded. SNP data were further filtered in the R library GenABEL v1.8-0 (Aulchenko *et al.* 2007) in R v3.6.3 with the *check.marker* function, retaining SNPs with call rates > 0.9 and individuals with call rates > 0.8. We did not filter SNPs that deviated from Hardy-Weinberg expectation. After QC, we retained 180,817 SNPs, which we hereafter refer to as the 180K

dataset. The SNP density on autosomes was 1 SNP every 5.1kb on autosomes, and 1 SNP every 206kb on the X chromosome. We investigated the linkage disequilibrium (LD) decay profile for each chromosome for all loci occurring within 500kb with each other using the flag *--ld-window-kb 500* in PLINK v1.90. LD decayed to $r^2 = 0.05$ at a distance of ~100kb, with LD decay slightly faster for micro-chromosomes (Figure S1).

SNP Quality Control for crossover estimation: When estimating recombination rate, any genotyping errors can cause problems when determining the grandparental origin of alleles. This can lead to false calling of double crossovers, resulting in an overestimation of recombination rate. Given that crossovers are inherently rare, false calling of double crossovers can have substantial downstream consequences on the analysis. For this reason, we conducted a second, more stringent quality control on the 200K dataset for crossover estimation. SNPs were filtered for Mendelian errors in plink and loci with a minor allele frequency of < 0.05 were discarded. For each SNP locus and individual, we extracted the raw allele intensity data from the Affymetrix Axiom genotyping project. These data were used to calculate the combined SNP intensity, *R*, and the allelic intensity ratio, Θ:

$$R = A + B \quad (1)$$

$$\Theta = \left(\frac{2}{\pi}\right) \times \arctan\left(\frac{B}{A}\right) \quad (2)$$

where A and B are the probe raw intensity values for each SNP allele in alphabetical order (e.g. C & T, respectively). These data generally cluster into the three genotypes separated by their Θ values (Figure S1). For each SNP locus, we calculated the mean and standard deviation of Θ for each genotype (i.e. for AA, AB and BB). After extensive visual examination of SNP clustering, we discarded any SNP locus where the standard deviation of Θ for any genotype was > 0.046. This threshold was selected as it ensured adequate cluster separation in the data and removed ambiguous genotypes occurring between clusters (see Figure S2 for a visual example). The remaining 63,535 SNPs were filtered to remove SNPs on the X chromosome, and those of unknown position; 61,180 SNPs were retained. We hereafter refer to this data set as the 61K dataset. This analysis was conducted in R v3.6.3.

Linkage mapping.

Autosomal linkage map construction and chromosome phasing was conducted using the 61K SNP dataset in CRI-MAP v2.504a (Green *et al.* 1990). To ensure unbiased phasing, a standard approach was used to quantify the crossovers occurring in individual gametes transmitted from parents to their offspring (Johnston *et al.* 2016). Hereafter, focal individual (FID) refers to the individual in which meiosis took place (i.e. the parent). For each FID-offspring pair, sub-pedigrees were constructed in each case where the FID, its parents, mate, and offspring were all genotyped (Figure S3), and then subject to the following quality control. First, Mendelian incompatibilities between parent and offspring genotypes were identified using the *prepare* function. Mendelian errors were then masked in both parents and offspring using the

create_crimap_input function in the package crimaptools v0.1 (https://github.com/susjoh/crimaptools, (Johnston *et al.* 2016)) implemented in R v3.6.3. Sub-pedigrees containing parent-offspring relationships with more than 0.1% mismatching loci were discarded. A total of 894 sub-pedigrees were used, representing 894 individual gametes transmitted from 368 unique FIDs. Sex-specific and sex-averaged linkage map positions in Kosambi centiMorgans (cM) were obtained for each chromosome using the *map* function, assuming SNPs were ordered as in the sparrow genome (Elgvin *et al.* 2017; Lundregan *et al.* 2018). SNPs for which both adjacent SNPs were greater than 3cM away in initial linkage maps were removed as they were assumed to be incorrectly mapped (132 SNPs). The *map* function was then re-run on the remaining 60,352 SNPs to produce the final linkage maps. Relationships between (a) chromosome length (in megabases) and linkage map length (in cM) and (b) male and female linkage map lengths (in cM) were analysed using linear regressions in R v3.6.3.

Calculating individual recombination rates.

Chromosome phasing and crossover estimation: The software YAPP v0.2a0 (https://yapp-doc.netlify.app/) (Servin 2021) was used to phase chromosomes and identify crossover (CO) positions. This approach used the whole pedigree rather than the smaller sub-pedigrees above, and is more robust to missing individuals, allowing us to characterise crossovers in more than three times the number of individual meioses (2,802 gametes transmitted from 972 FID). The 60,352 SNPs used in the CRIMAP linkage map analysis were filtered in PLINK prior to YAPP analysis using the *mendel* function with default parameters. This removed an additional 260 SNPS, with the remaining 60,092 used for phasing. The *phase* command was used to infer the gametic phase of chromosomes, and implements a Weighted Constraints Satisfaction Problem solver in the software ToulBar2 (Favier *et al.* 2018). Then, the *recomb* command was run to identify COs, with an additional parameter *--rho* defined as the chromosome recombination rate in cM/Mb. The *rho* parameter was to account for any variation in chromosome-wide recombination rate due to the large chromosomal size differences typical in the avian karyotype, and the constraint of obligate crossing over, which increases the cM/Mb ratio on smaller chromosomes. For each chromosome per meiosis, YAPP outputs the start and stop positions of the informative length of the chromosome (i.e. the total region where phase can be inferred, or “coverage”) and the start and stop positions of each crossover interval as determined by a Hidden Markov Model (Figure S4); this was included to account for CO detection being potentially reduced in individuals with lower coverage. We assumed that all COs are subject to interference and that short distances between double crossovers were indicative of phasing and/or genotyping errors. After visual examination of the distribution to determine an appropriate threshold, we removed all COs that were less than 2Mb apart (from the right-hand boundary of the first CO interval to the left-hand boundary of the second CO interval; Figure S4). In cases of clustered short COs (i.e. 3 or more adjacent COs that are separated by distances of 2Mb or less), 1 CO was called in the case of odd numbers of COs (i.e. a phase change occurred at either side of the cluster, or 0 COs in the case of even numbers of COs (i.e. there was no phase change on either side

of the cluster). Using YAPP, we phased 2,802 gametes transmitted from 494 unique male and 478 unique female FIDs, identifying a total of 49,212 COs.

Recombination rate calculation: The CO dataset was used to calculate recombination rates in FIDs using several approaches. First, we determined the autosomal crossover count (ACC) by summing the number of crossovers per gamete. Second, we calculated the rate of intra-chromosomal allelic shuffling, $\bar{r}_{intra}$, which is the probability that two randomly chosen loci (or genes) are on the same chromosome are uncoupled in meiosis (Veller *et al.* 2019). This was defined as:

$$\bar{r}_{intra} = \sum_{k=1}^{n} 2p_k(1-p_k)L_k^2$$

where for chromosome *k*, *p* is the proportion of the chromosome (or genes) from one parent, *L* is its fraction of the genome length (or gene count), and *n* is the autosome count. We define $\bar{r}_{genome}$ and $\bar{r}_{gene}$ as $\bar{r}_{intra}$ measures calculated with chromosome and gene proportions, respectively. To test the broader effects of chromosomes size, we then subset each ACC and $\bar{r}_{intra}$ measure as follows. First, measures were compiled from CO information on macro-chromosomes, here defined as all chromosomes greater than 19Mb in length (chromosomes 1:12 and 1A). Second, measures were compiled without micro-chromosomes, here defined as those with linkage maps of <50cM or physical maps of <10Mb (chromosomes 21 to 28), as they rarely have more than one crossover, and several of them do not meet the expectation of a minimum map length of 50cM (i.e. an obligate crossover), meaning that some crossovers are likely to be undetected. Therefore, all analyses of recombination rates were conducted on chromosomes 1A and 1 to 20, only. It should be noted that pedigree-based methods to estimate COs can only identify crossovers present in one of the four cells resulting from meiosis. For each CO, there will be two recombinant and two non-recombinant chromatids at that position. Therefore, our CO counts represent a sample of the crossovers that happened in meiosis I. We assume that each CO is sampled with a 50:50 probability, but we cannot rule out that meioses with two or more COs on the same chromosome may be more likely to be co-inherited on the same chromatid.

Determining Heritability of Recombination Rate.

The proportion of phenotypic variance in recombination measures attributed to additive genetic effects (narrow-sense heritability h^2) was determined using a restricted maximum-likelihood “animal model” in the package ASReml-R v4 (Butler *et al.* 2009) in R v4.2.2. A genomic relatedness matrix (GRM) at all autosomal markers within the 180K SNP dataset was constructed with GCTA v1.94.1 (Yang *et al.* 2011). The GRM was adjusted for sampling error using the *--grm-adj 0* argument, which assumes the frequency spectra of genotyped and causal loci are similar. Models were run for ACC, $\bar{r}_{genome}$ and $\bar{r}_{gene}$ in both sexes, and in males and females separately. The fixed effect structure included phase coverage from YAPP (the length of the genome that can be phased and therefore within which crossovers can be detected), parent sex as a fixed factor, and age of the FID in year of gamete formation (defined as the

difference between offspring hatch year and parent hatch year). For models of $\bar{r}$, we fit ACC as an additional fixed effect, as intra-locus shuffling is a function of the crossover count. Random effects included the additive genetic effect (GRM), permanent environment effect (repeated measures in each FID), and FID hatching year, FID island and offspring hatch year (to investigate cohort effects and parse apart environmental effects) and FID mother (to estimate maternal effects). The significance of random effects was determined from the Z ratio using the *pnorm* function in R. The heritability of each measure was determined as the ratio of the additive genetic variance to the total phenotypic variance (i.e. the sum of random effect variances and the residual variance). Bivariate models were run to determine the genetic correlation between male and female measures with coverage as a fixed effect. The additive genetic correlation, r_A, was calculated without constraint using the CORGH function (i.e. correlation with heterogenous variances) in ASReml-R v4. The significance of the correlation estimate was determined using the reported Z-ratio with 1 degree of freedom.

Determining Genomic Variants Associated with Recombination Rate.

***Genome-wide association studies (GWAS)*:** GWAS of recombination measures were conducted with the 180K SNP dataset using RepeatABEL v1.1 (Rönnegård *et al.* 2016) in R v3.6.3. Models were run for ACC, $\bar{r}_{genome}$ and $\bar{r}_{gene}$ in both sexes, and in males and females separately. The package models the additive effect of SNPs, where genotypes correspond to 0, 1 and 2, and slopes and standard errors of associations are calculated. To account for inflation of test statistics due to cryptic population structure, a relatedness matrix accounting for family structure was fit using the van Raden method (VanRaden 2008) implemented within RepeatABEL. To account for any further inflation, we divided association statistics using the genomic control parameter λ, which was calculated as the observed median χ^2 statistic, divided by the null expectation median χ^2 statistic (Devlin and Roeder 1999). The significance threshold was calculated using a Bonferroni correction, where the threshold at $\alpha = 0.05$ of $P = 2.765 \times 10^{-7}$.

Distribution of polygenic effects: We determined the distribution of allele effect sizes and false discovery rates (i.e. loci with non-zero effects on recombination rates) using the *ash* function in the R package ashR v2.2-32 (Stephens 2017). This package models the slopes and standard errors of the additive SNP effects from the GWAS in an Empirical Bayes framework to compute a posterior distribution of SNP effect sizes across all loci. For SNPs estimated to have non-zero effects on the trait, the significance of a SNP effect is determined by a local false sign rate, defined as probability of error when classifying the slope of the effect as positive or negative, with cut-off thresholds at $\alpha = 0.05$ and $\alpha = 0.01$. The prior distribution was specified to be any symmetric unimodal distribution when applying the false discovery rate estimation. We investigated functional enrichment in all annotated genes within 100kb of loci with non-zero effects on heritable traits using Panther v17.0 on the 2022-07-01 release of the GO Ontology database (DOI: 10.5281/zenodo.6799722) (Mi *et al.* 2021), using *Homo sapiens* and *Gallus* gallus as reference lists.

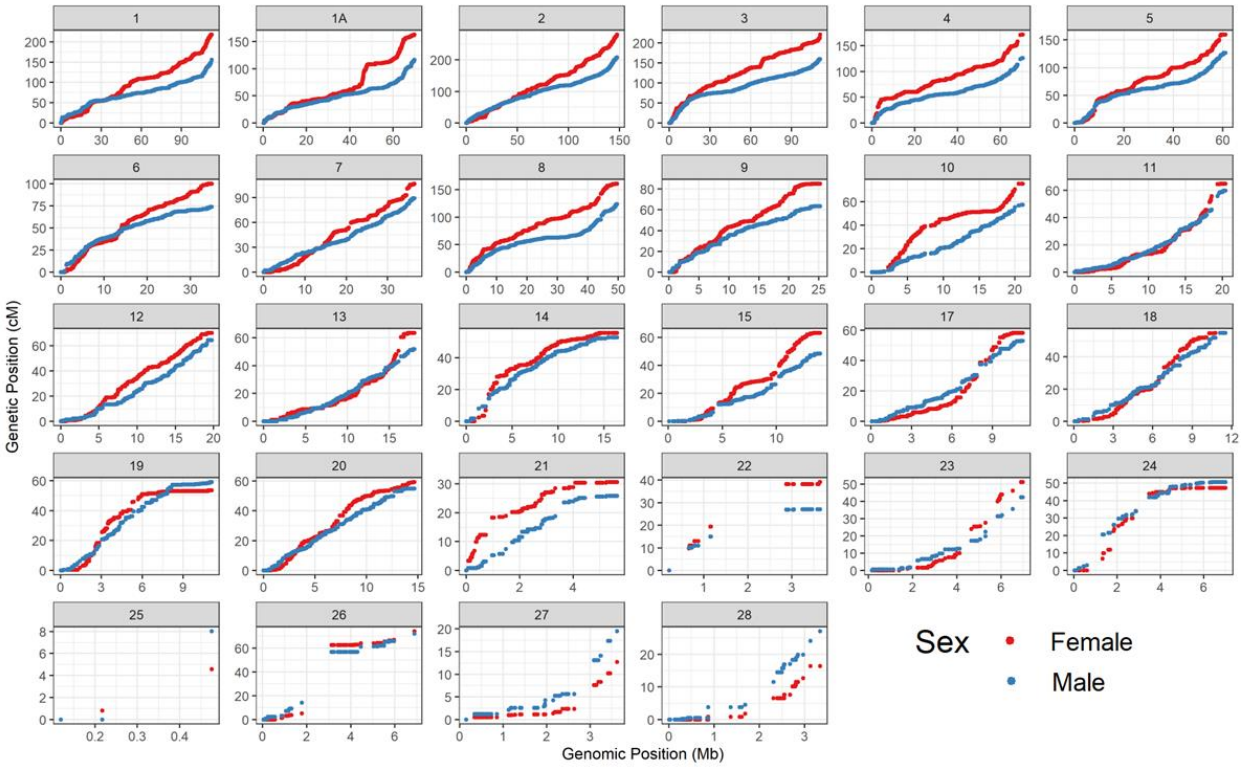

Figure 1: Sex-specific autosomal genetic linkage maps for house sparrows. Map summary data and full map positions are provided in Tables S1 and S2, respectively.

Results

Linkage Mapping.

We mapped 60,352 SNPs to 11,814 unique cM positions on 28 autosomal chromosomes, with some degree of heterogeneity in the landscape of recombination within and between the sexes (Figure 1, Table S1). The sex-averaged autosomal linkage map length was 2311.3cM, corresponding to a mean autosomal recombination rate of 2.53 cM/Mb. The female and male autosomal maps were 2558.1cM (2.8 cM/Mb) and 2069.6cM (2.26 cM/Mb), respectively. The female map length was 1.24 times longer than the male map length. There was a strong correlation between chromosome length and genetic map length ($r^2 = 0.946$, p < 0.0001; Figure 2A). Chromosome-wide recombination rate (cM/Mb) were higher in smaller autosomes ($r^2 = 0.749, p < 0.0001$, fitted as a logarithmic function), with microchromosomes demonstrating recombination rates 3 to 5 times that of the genome-wide average (Figure 2B). The degree of sex differences in recombination rate based on autosome length in centimorgans, was female biased for most linkage groups ($r^2 = 0.985, p < 0.0001$) (Figure 2C, Table S1). Chromosomes 21 to 28 (but not 26) had linkage map lengths of < 50cM, indicating that the obligate crossover cannot be picked up on those chromosomes. Summary statistics for map lengths are provided in Table S1, and the full linkage map is provided in Table S2.

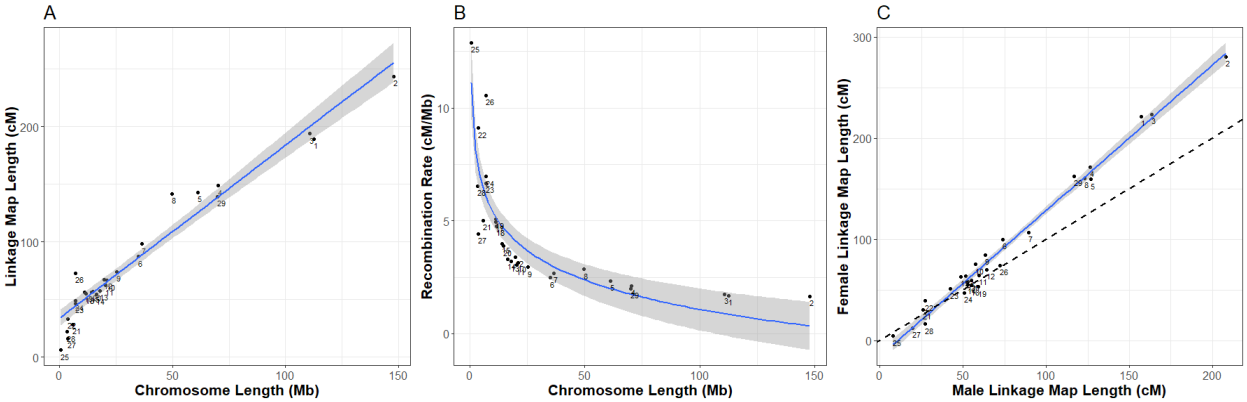

Figure 2. Variation in recombination rates between chromosomes, showing correlations between (A) the sex-averaged linkage map length (cM) and chromosome length (Mb); (B) chromosomal recombination rate (cM/Mb) and chromosome length; and (C) male and female linkage map lengths, where the dashed line indicates the slope at which rates are equal. Points are chromosome numbers, and lines and the grey-shaded areas indicate the regression slopes and standard errors, respectively.

Recombination rate variation.

We identified 49,212 COs across 2,802 gametes from 494 unique male and 478 unique females. Larger chromosomes had more COs per gamete than small chromosomes, with chromosomes 1 and 2 having up to 5 COs per gamete in some cases (Figure 3). Chromosomes 10 to 20 generally had 50% non-recombinant chromosomes, likely reflective of crossover interference over these short chromosomes leading to a single obligate CO, which has a 50% chance of segregation into the gamete. Chromosomes 21 to 28 had more than 50% of chromosomes with no COs, meaning that we had low power to pick up COs. Therefore, we removed these from all subsequent analyses and all results are reported from chromosomes 1A and 1 to 20. The autosomal crossover count (ACC) was 1.37 times higher in females than in males, with mean ACCs of 18.25 and 13.35, respectively (Figure 4). The rate of intra-chromosomal shuffling $\bar{r}_{intra}$ was 1.54 times and 1.46 times higher in females for $\bar{r}_{genome}$ and $\bar{r}_{gene}$, respectively (Figure 4). The distributions of ACC, $\bar{r}_{genome}$ and $\bar{r}_{gene}$ are shown in Figure S5. ACC and $\bar{r}_{genome}$ were highly positively correlated ($r^2 = 0.684$, $P < 0.0001$; Figure S6), and $\bar{r}_{genome}$ and $\bar{r}_{gene}$ were very highly positively correlated ($r^2 = 0.949$, $P < 0.001$).

Heritability and genome-wide association of recombination rates.

For all models of ACC, $\bar{r}_{genome}$ and $\bar{r}_{gene}$, only fixed effects of sex, total coverage, and total coverage^2 were significant (Table S3), as were only the additive genetic, permanent environment and residual random effects (Table 1). Henceforth, all results are from models with this fixed and random effect structure; full results of all models tested are provided in Supplementary File 1. ACC was heritable in both sexes ($h^2 = 0.091$) and females ($h^2 = 0.226$), but not in males ($h^2 = 0.036$, $P > 0.05$, Table 1). The additive genetic correlation between the sexes was not significantly different from zero ($r_A = 0.209$, Table 1), although this was expected when the trait is not heritable in one sex. The significant permanent

Table 1: Proportions of phenotypic variance explained by additive genetic (h^2), permanent environment effect (pe^2) and residual variance. V_P and V_P (obs) are the phenotypic variance as estimated from the animal model and from the raw data, respectively. Values in parentheses are the standard errors. Significance of each random effect is indicated by * (P < 0.05), ** (P < 0.001) and (P < 0.001). All results are from 2,802 gametes from 970 individuals, with 1,341 gametes from 477 females and 1,456 gametes from 493 males.

Rate Measure	Sex	V_P	V_P (Obs)	Mean	h^2	pe^2	r^2
ACC	Both	16.93	23.47	15.71	0.091	0.124	0.785
		(0.493)			(0.026)	(0.029)	(0.022)
	Female	23.35	24.52	18.26	**0.226**	0.041	0.733
		(1.031)			(0.054)	(0.048)	(0.033)
	Male	10.66	11.05	13.37	0.036	0.049	0.915
		(0.401)			(0.027)	(0.036)	(0.027)
$\bar{r}_{genome}$	Both	3.95×10^{-5}	7.97×10^{-5}	0.0214	**0.066**	2.79×10^{-5}	0.934
		(1.08×10^{-6})			(0.016)	(7.61×10^{-7})	(0.016)
	Female	3.65×10^{-5}	5.68×10^{-5}	0.0261	0.024	1.96×10^{-5}	0.976
		(1.42×10^{-6})			(0.019)	(7.61×10^{-7})	(0.019)
	Male	4.09×10^{-5}	6.06×10^{-5}	0.0170	0.075	0.013	0.911
		(1.56×10^{-6})			(0.035)*	(0.035)	(0.027)
$\bar{r}_{gene}$	Both	8.53×10^{-6}	2.48×10^{-5}	0.0146	**0.062**	0.013	0.925
		(2.33×10^{-7})			(0.020)**	(0.023)	(0.019)
	Female	8.19×10^{-6}	2.48×10^{-5}	0.0175	0.037	0.000	0.963
		(3.18×10^{-7})			(0.020)	(0.000)	(0.020)
	Male	8.43×10^{-6}	1.66×10^{-5}	0.0119	0.073*	0.021	0.906
		(3.21×10^{-7})			(0.036)	(0.037)	(0.027)

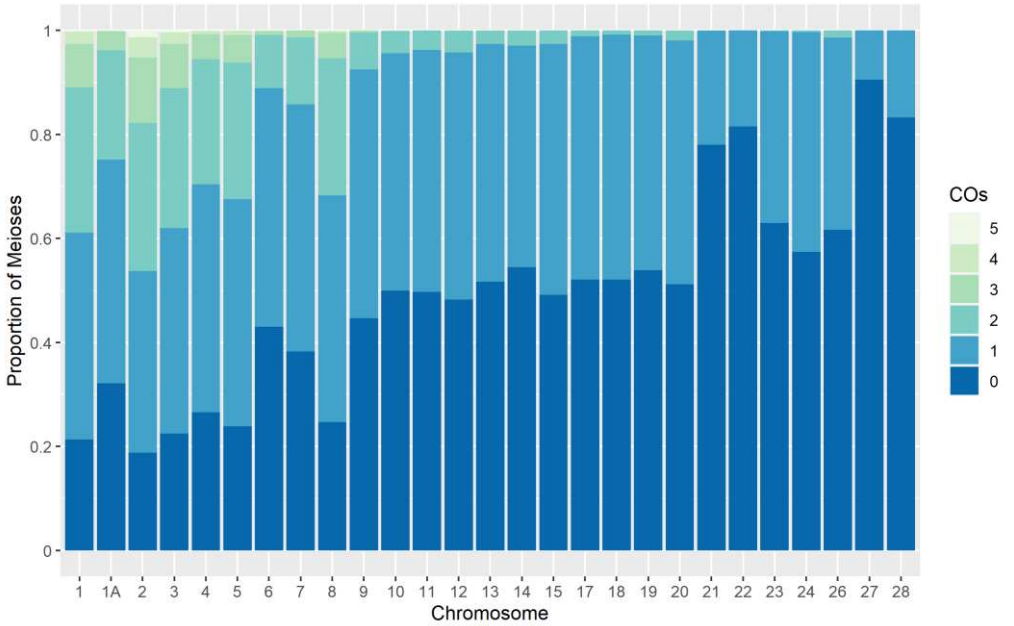

Figure 3: Distribution of CO counts per chromosome as the proportion of total number of gametes (N = 2,802).

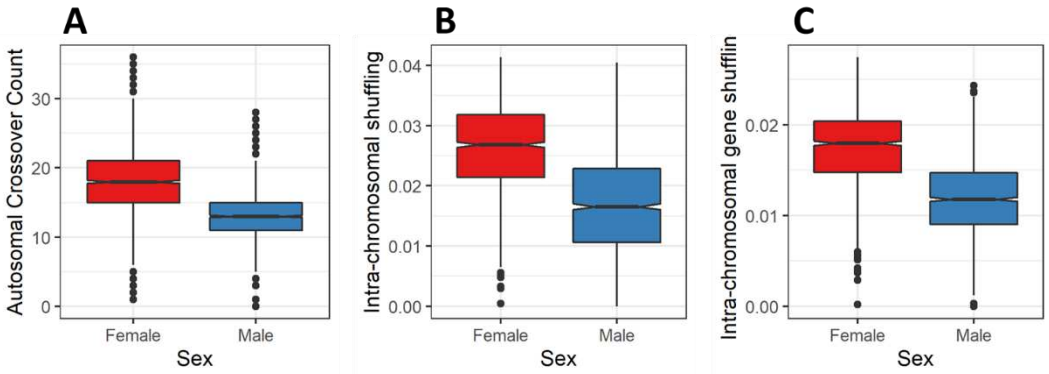

Figure 4. Boxplots of the distribution of female and male recombination rates. A) ACC, the total autosomal crossover count; B) $\bar{r}_{genome}$, the rate of intra-chromosomal shuffling as proportion of the genome; and C) $\bar{r}_{gene}$ the rate of intra-chromosomal shuffling of genes. Recombination rates are estimated for each FID and offspring pair, and indicate the rates of ACC and $\bar{r}$ in the gamete transmitted from the FID to their offspring.

environmental effect for both sexes (pe^2 = 0.124) may be an artefact, due to difficulties in partitioning the additive genetic component between groups when there is no genetic variance in one of them. The intra-chromosomal shuffling measures $\bar{r}_{genome}$ and $\bar{r}_{gene}$ were not heritable in females, but were heritable in males (h^2 = 0.075 and 0.073, respectively). The additive genetic correlation between the sexes could not be estimated for $\bar{r}_{genome}$ and $\bar{r}_{gene}$ as models could not converge without error, most likely due to the lack of heritable variation in females.

Genome-wide association studies and distribution of effect sizes.

Genome wide association studies in both sexes, females and males did not identify any loci that were significantly associated with variation in ACC, $\bar{r}_{genome}$ or $\bar{r}_{gene}$ (Figure 5, Figure S7). Empirical Bayes analysis of the GWAS summary statistics for heritable traits showed that 3,345 SNPs (1.8%) and 14 (0.008%) SNPs had non-zero effects on female ACC and male $\bar{r}$ at the level of α = 0.05, respectively (Figure S8). When considering α = 0.01, this reduced to 759 and 0 SNPs, respectively (Figure 6). Genes occurring within 100Kb of GWAS hits (1,151 genes) showed did not show functional enrichment for any processes related to meiosis, with the highest enrichment for nucleotide metabolic processes (1.83 times). Genes in regions associated with male $\bar{r}$ (20 genes) showed no functional enrichment. We noted that 5 of the 14 non-zero SNPs occurred from 53,319,263 to 53,465,310 on chromosome 1A in a region ~200Kb downstream of the Synaptonemal Complex Central Element Protein 3 (*SYCE3*).

Discussion

In this study, we have shown that female house sparrows have 1.37 times higher autosomal crossover counts (ACC) and ~1.5 times more intra-chromosomal shuffling ($\bar{r}_{intra}$) than males. ACC was moderately

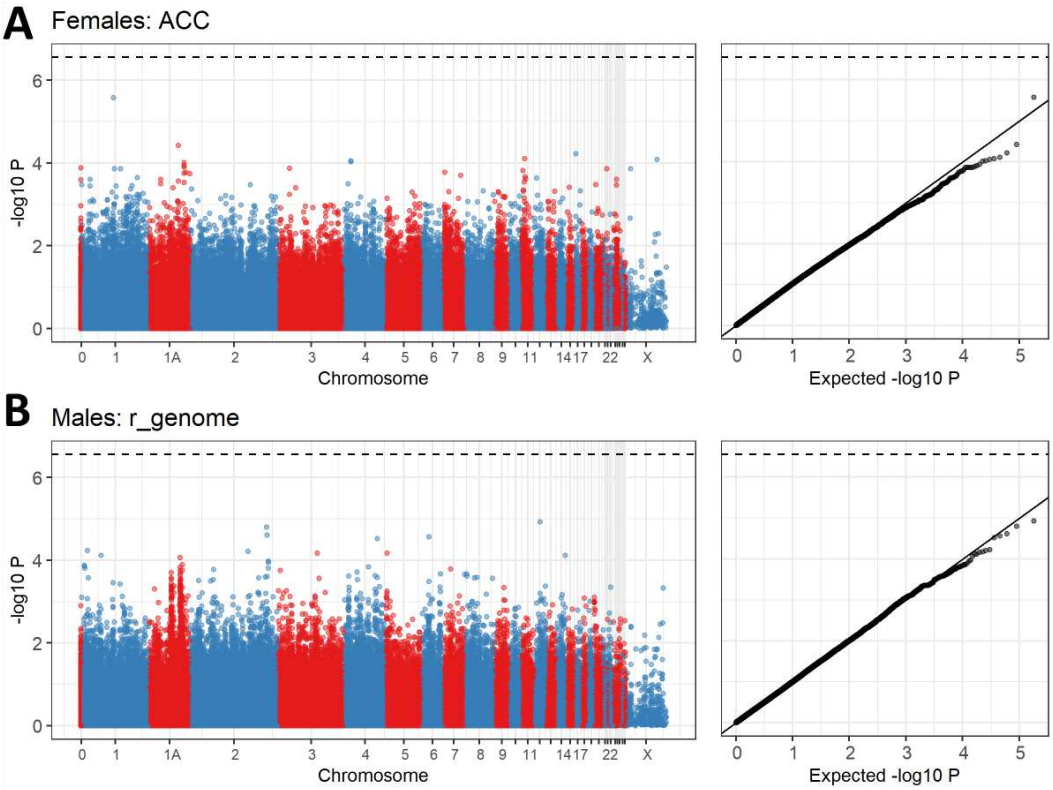

Figure 5: Manhattan and P-P plots for A) female autosomal crossover count (ACC) and B) male intra-chromosomal genome shuffling ($\bar{r}_{genome}$). The dashed line is the genome-wide significance equivalent to α = 0.05. Points have been colour-coded by chromosome. The right-hand column shows the distribution of P values against those under the null expectation. Association statistics have been corrected with the genomic control parameter λ. Sample sizes are given in Table 2. **NB**. Visually, P values on the X chromosome appear to be lower than on other chromosomes. This is an artefact of over-plotting of much higher marker densities on the other chromosomes, and association statistics are not significantly lower on the X chromosome.

heritable in females (h^2 = 0.23), whereas $\bar{r}$ was slightly heritable in males (h^2 = 0.07). A genome-wide association study found no regions of the genome with a significant effect on recombination rate, but that around 1.8% of SNPs in females had non-zero effect on ACC. Therefore, we conclude that the heritable variation recombination rate is polygenic and driven by many loci of small effect sizes. In males, this was less conclusive, with only 14 SNPs showing non-zero effects on $\bar{r}_{intra}$. Here, we discuss in more detail the variation in crossover count and intra-chromosomal shuffling, suggest hypotheses on the nature of polygenic variation in these measures, and the patterns that may contribute to the observed sexual dimorphism suggest several hypotheses to explain the observed genetic architecture within this sparrow population.

Trends and comparisons in linkage mapping.

Our main motivation for constructing a linkage map was to ensure that the SNPs used in estimation of recombination rates were correctly mapped, as any wrongly mapped SNPs could lead to false calling of crossovers in the individual rate analysis. Furthermore, if a wrongly-mapped marker has differences in phase informativeness that covaries with genotype, this could lead to false signals of individual differences at that SNP and potentially, false associations in a GWAS. Therefore, this was a necessary step in our study. Our higher-density linkage maps showed strong concordance with a recent 6.5K map in the same population (Hagen *et al.* 2020), although our map was 14% longer. It may be that our map has improved resolution at telomeric regions and microchromosomes to pick up more COs where recombination rates tend to be higher, and having more power to detect double crossovers. On the other hand, our use of the genome sequence to order our markers may introduce some upward bias if there are short rearrangements and/or misassembled regions. If this were the case, we can argue that the Hagen *et al.* map may be less sensitive to bias over the broad scale, and therefore more appropriate for comparative studies of recombination landscapes.

Our map confirmed heterogeneity in the recombination landscape, particularly between the sexes, where some regions showed strong divergence in rates (e.g. at ~45Mb on chromosome 1A, or 15-17.5Mb on chromosome 10, among others; Figure 1). These sex differences indicate that sudden changes in landscape are not necessarily indicative of rearrangements (i.e. when the other sex does not show the same trend), but they could indicate the positions of broader landscape features, such as centromeres, where males and females can have pronounced heterochiasmy (i.e. differences in male and female rates). As yet, the positions of centromeres remain unknown in the sparrow genome, but future work will investigate how recombination rate variation, particularly between the sexes, correlated with genomic features. Our overall recombination rate of 2.53 cM/Mb was concordant with recombination rates estimated based on cytogenetic analysis of chiasma counts in birds, which range from 1.6 cM/Mb in female common terns (*Sterna hirundo*; Lisachov *et al.* 2017) to 2.9 cM/Mb in female domestic geese (*Anser anser*; Torgasheva and Borodin 2017; see data compiled in Malinovskaya *et al.* 2018) and Table S5). There is slightly less concordance with previous linkage maps, particularly with those carried out with low marker densities in the early days of linkage mapping, where cM map lengths could be as low as 694cM for e.g. male Siberian jays (Jaari *et al.* 2009). It may be that marker densities in these cases have led to underestimation of recombination by having low sub-telomeric coverage or by being too widely spaced to quantify double crossovers. Therefore, understanding how landscapes of recombination vary relative to other avian species requires generation of higher density linkage maps in a wider range of systems.

Variation in crossover count and intra-chromosomal shuffling.

Much of the theory proposed to explain the advantages and disadvantages of recombination rate variation centres around the generation and preservation of beneficial haplotypes through shuffling of alleles at linked sites (Hill and Robertson 1966; Felsenstein 1974; Kondrashov 1988). The efficacy and extent to which crossovers shuffle linked alleles within chromosomes is not only a function of CO count, but also of the CO position (Veller *et al.* 2019). For example, a crossover in close proximity to a chromosome end will lead to much less allele shuffling than one in the centre of a chromosome (Veller *et al.* 2019). However, almost all previous studies investigating the genetic architecture of recombination rates have focussed solely on autosomal crossover counts (e.g. (Kong *et al.* 2014; Ma *et al.* 2015; Johnston *et al.* 2016; Petit *et al.* 2017)). In our study, we modelled both ACC and $\bar{r}_{intra}$ to consider two different (but not independent) phenomena, that respectively represent more the variation in the mechanistic process of CO formation (ACC) and the variation in the evolutionary consequences of recombination ($\bar{r}_{intra}$). We identified a substantial correlation between ACC and $\bar{r}$ (r^2 = 0.684), reflecting that the majority of variation in $\bar{r}_{intra}$ is driven by ACC, whereas the remainder may be due to other factors, such as individual differences in chromatin landscape, differences in the genetic architecture, and/or random processes that affect CO positioning. Interpreting $\bar{r}_{intra}$ is somewhat relative; we observe individual variation in males, where $\bar{r}_{intra}$ is heritable, and we also observe substantial differences in the amount of allele shuffling between the sexes. Females demonstrate higher ACC and $\bar{r}_{intra}$ than males, but this difference is stronger in terms of allele shuffling rather than the number of COs (~1.5× vs 1.37×, respectively). Therefore, females may exhibit a stronger capacity to drive responses to selection than males in this population, although in reality, it may be that the sex-averaged rate is more meaningful in terms of longer-term responses to selection (Burt *et al.* 1991). We discuss more about the implications of our findings on understanding sex differences in recombination below. Finally, our observation that ACC is heritable in females, but that $\bar{r}_{intra}$ is not, suggests that CO positioning in females may be more random across the genome.

One limitation of our method to characterise COs using pedigree information is that we only use data from gametes that resulted in an (adult) offspring. This leads to a “missing fraction” of recombination measures in the population, meaning that our measured rates may not be reflective of the true rate of crossing over during meiosis; for example, problems in meiosis and crossing over can translate into lower fertility and increased rates of aneuploidy in humans (Hassold and Hunt 2001; Kong *et al.* 2004; Handel and Schimenti 2010; MacLennan *et al.* 2015). This also causes problems for future analyses of fitness (i.e. FID reproductive success, and offspring viability) as rates are already biased towards having more surviving offspring. This bias is likely to persist even with genomic measures, for example, if we were to estimate breeding values for recombination rate using genomic prediction in individuals without surviving offspring (Meuwissen *et al.* 2001). Currently, we are overcoming this by genotyping thousands of hatched individuals to gain a better understanding of variation in recombination and its relationship with offspring

fitness post-zygotically. However, a full understanding of the missing fraction would aim to characterise variation at the pre-zygotic stage e.g. by verifying rate variation using chiasma count data (Malinovskaya *et al.* 2020b).

What is the nature of polygenic variation underpinning recombination rates?

The mammal studies of recombination outlined in the introduction consistently find modest levels of heritable variation, most often higher in females, and identify a conserved suite of loci (e.g. *RNF212*, *RNF212B*, *REC8*, *MSH4*, *HEI10*, among others) that explain a moderate to large effect of heritable variation in ACC (Kong *et al.* 2014; Kadri *et al.* 2016; Petit *et al.* 2017; Johnston *et al.* 2018; Brekke *et al.* 2022a). In our study, we identify substantial heritability for female ACC (h^2 = 0.23) and male $\bar{r}_{intra}$ (h^2 = 0.07), but unlike mammal studies, we show compelling evidence that this variation is polygenic and driven by many loci of small effect throughout the genome. Understanding the nature of this polygenic variation will require further investigation. Indeed, recombination rate is an unusual trait to model in a GWAS, as we must consider that SNPs may be in LD with genomic features that contribute to regulation of recombination rate variation in *cis* (e.g. polymorphic hotspots) and protein coding regions that affect recombination rate in *trans* (i.e. global modifiers of recombination, as demonstrated in the mammal studies above). In future studies investigating fine-scale variation in recombination across the genome, *cis* vs *trans* effects could be tested by investigating the correlation between regions with non-zero effects and local variance in recombination rates, or by estimating the variance explained by a chromosome for its own recombination rate, vs how much intra-chromosomal variance is explained by all other chromosomes.

Another factor that may contribute to heritable variation is the presence of the germline-restricted chromosome (GRC) in female birds (Torgasheva *et al.* 2019; Borodin *et al.* 2022). This large chromosome was discovered in the late 1990s, is likely present in all passerines, can comprise around 10% of the genome, but is not present in somatic cells (Pigozzi and Solari 1998; Warren *et al.* 2010). In males, it is generally ejected before meiosis, whereas in females it duplicates and forms crossovers with itself (Malinovskaya *et al.* 2020a; Pei *et al.* 2022). The function and evolution of the GRC is still poorly understood, but recent work has shown that it is enriched for genes for germline development and that its gene content may differ between species (Kinsella *et al.* 2019). Therefore, we cannot rule out that additive genetic variance for female ACC, a process that takes place in cells that contain GRCs, could be partially or fully explained by genetic variation on the GRC. As related females may be more likely to carry more genetically similar GRCs, then this would be captured in the genomic relatedness matrix in our animal models above, but would not be captured by SNP array variation as this only targets somatic genomes. Investigating this contribution will be highly challenging, but future research in this area may provide the power and possibility to test this hypothesis. Finally, whilst the marker density we used here is high relative to the observed decay in linkage disequilibrium, we acknowledge that a lack of association

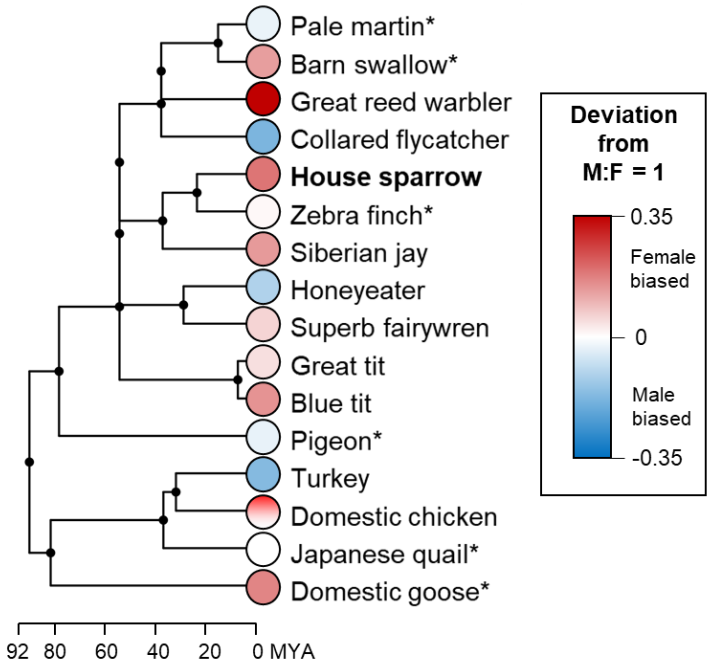

Figure 6: Phylogeny of birds where within sex recombination rates have been estimated using linkage mapping, or cytogenetic analysis of chiasma counts using MLH1 foci or recombination nodules (indicated by *). The underlying data is provided in Table S5 using data compiled in (Malinovskaya *et al.* 2020b) and other sources. This figure should be taken as illustrative - we note that some of the linkage map data is likely to have had poor marker densities in telomeric regions and have less resolution to detect double crossovers. As recombination landscape and crossover rates are sex-dependent, this could underestimate recombination in one sex, hence why we have not made a formal comparison.

with GWAS can also arise due to reduced power to detect trait loci, due to relatively small sample sizes compared to human and livestock studies (Santure and Garant 2018; Johnston *et al.* 2022).

Sex Differences in Recombination.

This study provides a compelling example of sexual dimorphism in recombination rate and broad-scale landscapes. This phenomenon is known as heterochiasmy, and can differ in direction and degree even between closely related species (Lenormand and Dutheil 2005; Sardell and Kirkpatrick 2020; Cooney *et al.* 2021). As recently as 2006, it was stated that birds did not exhibit heterochiasmy, and that it was likely to be an extended feature across the clade (Calderón and Pigozzi 2006). Since then, linkage mapping and cytogenetic studies have challenged this assertion, by showing that heterochiasmy can be male or female biased and differ even within and between closely-related species (Figure 6; data and references in Table S5). However, absolute values of heterochiasmy in older linkage mapping studies should be interpreted with some caution, as low-density linkage map data in very early studies may have less resolution to detect double crossovers and telomeric COs, which in turn could bias estimates of heterochiasmy. With the exception of domestic chickens (Weng *et al.* 2019), our study is the largest study of individual variation in recombination in both sexes in birds. As the number of gametes from males and

females are similar in our study, and coverage is high across coding sequence, we are confident that we capture the vast majority of biologically meaningful COs.

A number of broad trends in sex-differences have been observed, such as females tending to have higher rates and more recombination near centromeres (Brandvain and Coop 2012). A number of hypotheses have been proposed to explain these trends (Sardell and Kirkpatrick 2020). For example, Trivers (1988) postulated that the sex under stronger selection should reduce recombination to preserve favourable haplotypes, whereas Felsenstein (1988) countered that it should have increased recombination to increase genetic variation in offspring fitness. Others suggested that selection for heterochiasmy operates at the gametic level (e.g. Nei 1969); Lenormand (2003) used an in-depth theoretical model of different evolutionary scenarios, concluding that the most plausible explanation is that the sex experiencing the more intense haploid selection (e.g. male vertebrates) should recombine less (Lenormand and Dutheil 2005). Brandvain and Coop (2012) proposed that higher recombination around female centromeres can reduce the effects of centromeric meiotic drive exploiting the asymmetry of female meiosis. Finally, Burt *et al.* (1991) suggested that that sex-specific rates may not be under selection, but that selection ultimately acts on the sex-averaged rate of recombination. Despite this rich literature and several comparative investigations (Lenormand and Dutheil 2005; Mank 2009; Cooney *et al.* 2021), there is still little support for different hypotheses. While we cannot directly relate heterochiasmy in a single population to a particular hypothesis, our results add to a growing body of data that there is sexual dimorphism in not only the rate of crossing over, but also in its positioning and in its genetic architecture. Our data show that there is potential for sex-differences in recombination rates to evolve in this population through genetic variation for female ACC and male $\bar{r}_{intra}$.

Conclusions.

In this study, we show sex differences in landscapes, rates and the genetic architecture of recombination in wild house sparrows. This study is a first step to investigating the selective and evolutionary importance of recombination in wild birds, with future analyses investigating fine-scale variation in recombination rate, and association between recombination rates and fitness effects. Our results expand our understanding of individual variation in recombination in a non-mammal system and our approach has the potential to be extended to other long-term studies with genomic, pedigree, and fitness information.

Acknowledgements

We thank students and fieldworkers for help with fieldwork, and the hospitality of inhabitants at the study area in Helgeland who made this study possible. Sampling was conducted in accordance with permits from the Norwegian Food Safety Authority and the Ringing Centre at Stavanger Museum, Norway. We thank Cathrine Brekke, Mark Ravinet, Jarrod Hadfield, Alexander Suh, Anna Torgasheva, Anna Runemark, Homa Papoli Yazdi, Martin Stoffel, and Anna Hewett for helpful discussions on this topic. The

house sparrow field study and genomic resource development was funded by the Research Council of Norway (RCN grant nos. 221956, 274930 and 302619), and the RCN's Centres of Excellence funding scheme (grant no. 223257). S.E.J. was funded by a Royal Society University Research Fellowship (grant nos. UF150448 and URF/R/211008). J.B.M. was funded by a Darwin Trust of Edinburgh PhD studentship.

AUTHOR CONTRIBUTIONS

S.E.J. & H.J. conceived and designed the study. H.J. and T.H.R. organised and collected field data. H.J., A.H., I.H. & A.K.N. generated the genomic dataset. J.B.M. & S.E.J. analysed the data. B.S. developed and modified the YAPP software for the analysis. L.P. conducted the *ashR* analysis. J.B.M. & S.E.J. wrote the manuscript with input from all authors.

DATA STATEMENT

Data will be archived when submitted. All scripts will be available at the following link for review: https://github.com/sejlab/Sparrow_Indiv_Recomb_McAuley

Referenced Literature

Anderson T. R., 2006 *Biology of the Ubiquitous House Sparrow: From Genes to Populations*. Oxford University Press., Oxford, UK.

Aslam M. L., J. W. M. Bastiaansen, R. P. M. A. Crooijmans, A. Vereijken, H.-J. Megens, *et al.*, 2010 A SNP based linkage map of the turkey genome reveals multiple intrachromosomal rearrangements between the turkey and chicken genomes. BMC Genomics 11: 647.

Aulchenko Y. S., S. Ripke, A. Isaacs, and C. M. van Duijn, 2007 GenABEL: an R library for genome-wide association analysis. Bioinformatics 23: 1294–1296.

Backström N., N. Karaiskou, E. H. Leder, L. Gustafsson, C. R. Primmer, *et al.*, 2008 A gene-based genetic linkage map of the collared flycatcher (Ficedula albicollis) reveals extensive synteny and gene-order conservation during 100 million years of avian evolution. Genetics 179: 1479–1495.

Baker Z., M. Schumer, Y. Haba, L. Bashkirova, C. Holland, *et al.*, 2017 Repeated losses of PRDM9-directed recombination despite the conservation of PRDM9 across vertebrates. Elife 6. https://doi.org/10.7554/elife.24133

Baudat F., J. Buard, C. Grey, A. Fledel-Alon, C. Ober, *et al.*, 2010 PRDM9 is a major determinant of meiotic recombination hotspots in humans and mice. Science 327: 836–840.

Borodin P., A. Chen, W. Forstmeier, S. Fouché, L. Malinovskaya, *et al.*, 2022 Mendelian nightmares: the germline-restricted chromosome of songbirds. Chromosome Res. 30: 255–272.

Brandvain Y., and G. Coop, 2012 Scrambling eggs: meiotic drive and the evolution of female recombination rates. Genetics 190: 709–723.

Brekke C., P. Berg, A. B. Gjuvsland, and S. E. Johnston, 2022a Recombination rates in pigs differ between breeds, sexes and individuals, and are associated with the RNF212, SYCP2, PRDM7, MEI1 and MSH4 loci. Genet. Sel. Evol. 54: 33.

Brekke C., S. E. Johnston, A. B. Gjuvsland, and P. Berg, 2022b Variation and genetic control of individual recombination rates in Norwegian Red dairy cattle. J. Dairy Sci. https://doi.org/10.3168/jds.2022-22368

Burt A., G. Bell, and P. H. Harvey, 1991 Sex differences in recombination. J. Evol. Biol. 4: 259–277.

Butler D. G., B. R. Cullis, A. R. Gilmour, and B. J. Gogel, 2009 *Mixed models for S language environments: ASReml-R Reference Manual*.

Calderón P. L., and M. I. Pigozzi, 2006 MLH1-focus mapping in birds shows equal recombination between sexes and diversity of crossover patterns. Chromosome Res. 14: 605–612.

Capilla L., N. Medarde, A. Alemany-Schmidt, M. Oliver-Bonet, J. Ventura, *et al.*, 2014 Genetic recombination variation in wild Robertsonian mice: on the role of chromosomal fusions and Prdm9 allelic background. Proc. Biol. Sci. 281: 20140297.

Charlesworth B., and N. H. Barton, 1996 Recombination load associated with selection for increased recombination. Genet. Res. 67: 27–41.

Cooney C. R., J. E. Mank, and A. E. Wright, 2021 Constraint and divergence in the evolution of male and female recombination rates in fishes. Evolution 75: 2857–2866.

Coop G., and M. Przeworski, 2007 An evolutionary view of human recombination. Nature Reviews Genetics 8: 23–34.

Devlin B., and K. Roeder, 1999 Genomic control for association studies. Biometrics 55: 997–1004.

Elgvin T. O., C. N. Trier, O. K. Tørresen, I. J. Hagen, S. Lien, *et al.*, 2017 The genomic mosaicism of hybrid speciation. Sci. Adv. 3: e1602996.

Favier A., J.-M. Elsen, S. de Givry, and A. Legarra, 2018 Optimal haplotype reconstruction in half-sib families, in EasyChair.

Felsenstein J., 1974 The evolutionary advantage of recombination. Genetics 78: 737–756.

Felsenstein J., 1988 Sex and the evolution of recombination, pp. 74–86 in *Evolution of Sex: An Examination of Current Ideas*, edited by Richard E. Michod B. R. L. Sinauer Associates Inc., Sunderland, Massachusetts.

Garagna S., J. Page, R. Fernandez-Donoso, M. Zuccotti, and J. B. Searle, 2014 The Robertsonian phenomenon in the house mouse: mutation, meiosis and speciation. Chromosoma 123: 529–544.

Green P., K. Falls, and S. Crooks, 1990 *Documentation for CRIMAP, Version 2.4*. Washington University School of Medicine, St. Louis, MO.

Grey C., F. Baudat, and B. de Massy, 2018 PRDM9, a driver of the genetic map. PLoS Genet. 14: e1007479.

Groenen M. A. M., P. Wahlberg, M. Foglio, H. H. Cheng, H.-J. Megens, *et al.*, 2009 A high-density SNP-based linkage map of the chicken genome reveals sequence features correlated with recombination rate. Genome Res. 19: 510–519.

Hagen I. J., S. Lien, A. M. Billing, T. O. Elgvin, C. Trier, *et al.*, 2020 A genome-wide linkage map for the house sparrow (Passer domesticus) provides insights into the evolutionary history of the avian genome. Mol. Ecol. Resour. 20: 544–559.

Halldorsson B. V., G. Palsson, O. A. Stefansson, H. Jonsson, M. T. Hardarson, *et al.*, 2019 Characterizing mutagenic effects of recombination through a sequence-level genetic map. Science 363: eaau1043.

Handel M. A., and J. C. Schimenti, 2010 Genetics of mammalian meiosis: regulation, dynamics and impact on fertility. Nat. Rev. Genet. 11: 124–136.

Hansson B., M. Akesson, J. Slate, and J. M. Pemberton, 2005 Linkage mapping reveals sex-dimorphic map distances in a passerine bird. Proc. Biol. Sci. 272: 2289–2298.

Hansson B., M. Ljungqvist, D. A. Dawson, J. C. Mueller, J. Olano-Marin, *et al.*, 2010 Avian genome evolution: insights from a linkage map of the blue tit (Cyanistes caeruleus). Heredity (Edinb.) 104: 67–78.

Hartfield M., and P. D. Keightley, 2012 Current hypotheses for the evolution of sex and recombination. Integr. Zool. 7: 192–209.

Hassold T., and P. Hunt, 2001 To err (meiotically) is human: the genesis of human aneuploidy. Nature Reviews Genetics 2: 280–291.

Hill W. G., and A. Robertson, 1966 The effect of linkage on limits to artificial selection. Genetical Research 8: 269–294.

Huisman J., 2017 Pedigree reconstruction from SNP data: parentage assignment, sibship clustering and beyond. Mol. Ecol. Resour. 17: 1009–1024.

Jaari S., M.-H. Li, and J. Merilä, 2009 A first-generation microsatellite-based genetic linkage map of the Siberian jay (Perisoreus infaustus): insights into avian genome evolution. BMC Genomics 10: 1.

Jensen H., B.-E. SAEther, T. H. Ringsby, J. Tufto, S. C. Griffith, *et al.*, 2004 Lifetime reproductive success in relation to morphology in the house sparrow Passer domesticus. J. Anim. Ecol. 73: 599–611.

Johnsson M., A. Whalen, R. Ros-Freixedes, G. Gorjanc, C.-Y. Chen, *et al.*, 2021 Genetic variation in recombination rate in the pig. Genet. Sel. Evol. 53: 54.

Johnston S. E., C. Bérénos, J. Slate, and J. M. Pemberton, 2016 Conserved Genetic Architecture Underlying Individual Recombination Rate Variation in a Wild Population of Soay Sheep (Ovis aries). Genetics 203: 583–598.

Johnston S. E., J. Huisman, and J. M. Pemberton, 2018 A Genomic Region Containing REC8 and RNF212B Is Associated with Individual Recombination Rate Variation in a Wild Population of Red Deer (Cervus elaphus). G3 8: 2265–2276.

Johnston S. E., N. Chen, and E. B. Josephs, 2022 Taking Quantitative Genomics into the Wild. Proc. Roy. Soc. B 289: 20221930.

Kadri N. K., C. Harland, P. Faux, N. Cambisano, L. Karim, *et al.*, 2016 Coding and noncoding variants in HFM1, MLH3, MSH4, MSH5, RNF212, and RNF212B affect recombination rate in cattle. Genome Res. 26: 1323–1332.

Kawakami T., L. Smeds, N. Backström, A. Husby, A. Qvarnström, *et al.*, 2014 A high-density linkage map enables a second-generation collared flycatcher genome assembly and reveals the patterns of avian recombination rate variation and chromosomal evolution. Mol. Ecol. 23: 4035–4058.

Kinsella C. M., F. J. Ruiz-Ruano, A.-M. Dion-Côté, A. J. Charles, T. I. Gossmann, *et al.*, 2019 Programmed DNA elimination of germline development genes in songbirds. Nat. Commun. 10: 5468.

Kondrashov A. S., 1988 Deleterious mutations and the evolution of sexual reproduction. Nature 336: 435–440.

Kong A., J. Barnard, D. F. Gudbjartsson, G. Thorleifsson, G. Jonsdottir, *et al.*, 2004 Recombination rate and reproductive success in humans. Nat. Genet. 36: 1203–1206.

Kong A., G. Thorleifsson, M. L. Frigge, G. Masson, D. F. Gudbjartsson, *et al.*, 2014 Common and low-frequency variants associated with genome-wide recombination rate. Nat. Genet. 46: 11–16.

Lenormand T., 2003 The evolution of sex dimorphism in recombination. Genetics 163: 811–822.

Lenormand T., and J. Dutheil, 2005 Recombination difference between sexes: a role for haploid selection. PLoS Biol. 3: e63.

Lisachov A. P., L. P. Malinovskaya, A. V. Druzyaka, P. M. Borodin, and A. A. Torgasheva, 2017 Synapsis and recombination of autosomes and sex chromosomes in two terns (Sternidae, Charadriiformes, Aves). Vavilovskii Zhurnal Genet. Selektsii 21: 259–268.

Lundregan S. L., I. J. Hagen, J. Gohli, A. K. Niskanen, P. Kemppainen, *et al.*, 2018 Inferences of genetic architecture of bill morphology in house sparrow using a high-density SNP array point to a polygenic basis. Mol. Ecol. 27: 3498–3514.

Ma L., J. R. O'Connell, P. M. VanRaden, B. Shen, A. Padhi, *et al.*, 2015 Cattle Sex-Specific Recombination and Genetic Control from a Large Pedigree Analysis. PLoS Genet. 11: e1005387.

MacLennan M., J. H. Crichton, C. J. Playfoot, and I. R. Adams, 2015 Oocyte development, meiosis and aneuploidy. Semin. Cell Dev. Biol. 45: 68–76.

Malinovskaya L., E. Shnaider, P. Borodin, and A. Torgasheva, 2018 Karyotypes and recombination patterns of the Common Swift (Apus apus Linnaeus, 1758) and Eurasian Hobby (Falco subbuteo Linnaeus, 1758). Avian Res. 9. https://doi.org/10.1186/s40657-018-0096-7

711 Malinovskaya L. P., K. S. Zadesenets, T. V. Karamysheva, E. A. Akberdina, E. A. Kizilova, *et al.*, 2020a
712 Germline-restricted chromosome (GRC) in the sand martin and the pale martin (Hirundinidae,
713 Aves): synapsis, recombination and copy number variation. Sci. Rep. 10: 1058.
714 Malinovskaya L. P., K. Tishakova, E. P. Shnaider, P. M. Borodin, and A. A. Torgasheva, 2020b
715 Heterochiasmy and sexual dimorphism: The case of the barn swallow (Hirundo rustica,
716 hirundinidae, Aves). Genes (Basel) 11: 1119.
717 Mank J. E., 2009 The evolution of heterochiasmy: the role of sexual selection and sperm competition in
718 determining sex-specific recombination rates in eutherian mammals. Genet. Res. (Camb.) 91:
719 355–363.
720 Meuwissen T. H., B. J. Hayes, and M. E. Goddard, 2001 Prediction of total genetic value using genome-
721 wide dense marker maps. Genetics 157: 1819–1829.
722 Mi H., D. Ebert, A. Muruganujan, C. Mills, L.-P. Albou, *et al.*, 2021 PANTHER version 16: a revised family
723 classification, tree-based classification tool, enhancer regions and extensive API. Nucleic Acids
724 Res. 49: D394–D403.
725 Muñoz-Fuentes V., M. Marcet-Ortega, G. Alkorta-Aranburu, C. Linde Forsberg, J. M. Morrell, *et al.*, 2015
726 Strong artificial selection in domestic mammals did not result in an increased recombination rate.
727 Mol. Biol. Evol. 32: 510–523.
728 Myers S., L. Bottolo, C. Freeman, G. McVean, and P. Donnelly, 2005 A fine-scale map of recombination
729 rates and hotspots across the human genome. Science 310: 321–324.
730 Myers S., R. Bowden, A. Tumian, R. E. Bontrop, C. Freeman, *et al.*, 2010 Drive against hotspot motifs in
731 primates implicates the PRDM9 gene in meiotic recombination. Science 327: 876–879.
732 Nei M., 1969 Linkage modifications and sex difference in recombination. Genetics 63: 681–699.
733 Niskanen A. K., A. M. Billing, H. Holand, I. J. Hagen, Y. G. Araya-Ajoy, *et al.*, 2020 Consistent scaling of
734 inbreeding depression in space and time in a house sparrow metapopulation. Proc. Natl. Acad.
735 Sci. U. S. A. 117: 14584–14592.
736 Oers K. van, A. W. Santure, I. De Cauwer, N. E. M. van Bers, R. P. M. A. Crooijmans, *et al.*, 2014
737 Replicated high-density genetic maps of two great tit populations reveal fine-scale genomic
738 departures from sex-equal recombination rates. Heredity (Edinb.) 112: 307–316.
739 Ortiz-Barrientos D., J. Engelstädter, and L. H. Rieseberg, 2016 Recombination rate evolution and the
740 origin of species. Trends Ecol. Evol. 31: 226–236.
741 Otto S. P., and N. H. Barton, 2001 Selection for recombination in small populations. Evolution 55: 1921–
742 1931.
743 Otto S. P., and T. Lenormand, 2002 Resolving the paradox of sex and recombination. Nat. Rev. Genet. 3:
744 252–261.
745 Pan J., M. Sasaki, R. Kniewel, H. Murakami, H. G. Blitzblau, *et al.*, 2011 A hierarchical combination of
746 factors shapes the genome-wide topography of yeast meiotic recombination initiation. Cell 144:
747 719–731.
748 Pardo-Manuel de Villena F., and C. Sapienza, 2001 Recombination is proportional to the number of
749 chromosome arms in mammals. Mamm. Genome 12: 318–322.
750 Pärn H., T. H. Ringsby, H. Jensen, and B.-E. Sæther, 2012 Spatial heterogeneity in the effects of climate
751 and density-dependence on dispersal in a house sparrow metapopulation. Proc. Biol. Sci. 279:
752 144–152.
753 Pei Y., W. Forstmeier, F. J. Ruiz-Ruano, J. C. Mueller, J. Cabrero, *et al.*, 2022 Occasional paternal
754 inheritance of the germline-restricted chromosome in songbirds. Proc. Natl. Acad. Sci. U. S. A.
755 119: e2103960119.
756 Peñalba J. V., Y. Deng, Q. Fang, L. Joseph, C. Moritz, *et al.*, 2020 Genome of an iconic Australian bird:
757 High-quality assembly and linkage map of the superb fairy-wren (Malurus cyaneus). Mol. Ecol.
758 Resour. 20: 560–578.

759 Petit M., J.-M. Astruc, J. Sarry, L. Drouilhet, S. Fabre, *et al.*, 2017 Variation in recombination rate and its
760 genetic determinism in sheep populations. Genetics 207: 767–784.
761 Pigozzi M. I., and A. J. Solari, 1998 Germ cell restriction and regular transmission of an accessory
762 chromosome that mimics a sex body in the zebra finch, Taeniopygia guttata. Chromosome Res.
763 6: 105–113.
764 Pigozzi M. I., and A. J. Solari, 1999 Equal frequencies of recombination nodules in both sexes of the
765 pigeon suggest a basic difference with eutherian mammals. Genome 42: 315–321.
766 Pigozzi M. I., 2001 Distribution of MLH1 foci on the synaptonemal complexes of chicken oocytes.
767 Cytogenet. Cell Genet. 95: 129–133.
768 Purcell S., B. Neale, K. Todd-Brown, L. Thomas, M. A. R. Ferreira, *et al.*, 2007 PLINK: a tool set for
769 whole-genome association and population-based linkage analyses. Am. J. Hum. Genet. 81: 559–
770 575.
771 Ranke P. S., Y. G. Araya-Ajoy, T. H. Ringsby, H. Pärn, B. Rønning, *et al.*, 2021 Spatial structure and
772 dispersal dynamics in a house sparrow metapopulation. J. Anim. Ecol. 90: 2767–2781.
773 Reynolds A., H. Qiao, Y. Yang, J. K. Chen, N. Jackson, *et al.*, 2013 RNF212 is a dosage-sensitive
774 regulator of crossing-over during mammalian meiosis. Nat. Genet. 45: 269–278.
775 Ritz K. R., M. A. F. Noor, and N. D. Singh, 2017 Variation in recombination rate: Adaptive or not? Trends
776 Genet. 33: 364–374.
777 Robledo-Ruiz D. A., H. M. Gan, P. Kaur, O. Dudchenko, D. Weisz, *et al.*, 2022 Chromosome-length
778 genome assembly and linkage map of a critically endangered Australian bird: the helmeted
779 honeyeater. Gigascience 11. https://doi.org/10.1093/gigascience/giac025
780 Rönnegård L., S. E. McFarlane, A. Husby, T. Kawakami, H. Ellegren, *et al.*, 2016 Increasing the power of
781 genome wide association studies in natural populations using repeated measures - evaluation
782 and implementation. Methods Ecol. Evol. 7: 792–799.
783 Ross-Ibarra J., 2004 The evolution of recombination under domestication: a test of two hypotheses. Am.
784 Nat. 163: 105–112.
785 Saatoglu D., A. K. Niskanen, M. Kuismin, P. S. Ranke, I. J. Hagen, *et al.*, 2021 Dispersal in a house
786 sparrow metapopulation: An integrative case study of genetic assignment calibrated with
787 ecological data and pedigree information. Mol. Ecol. 30: 4740–4756.
788 Santure A. W., and D. Garant, 2018 Wild GWAS—association mapping in natural populations. Mol. Ecol.
789 Resour. 18: 729–738.
790 Sardell J. M., and M. Kirkpatrick, 2020 Sex differences in the recombination landscape. Am. Nat. 195:
791 361–379.
792 Servin B., 2021 *YAPP: Yet Another Phasing Program*.
793 Singhal S., E. M. Leffler, K. Sannareddy, I. Turner, O. Venn, *et al.*, 2015 Stable recombination hotspots in
794 birds. Science 350: 928–932.
795 Stapley J., T. R. Birkhead, T. Burke, and J. Slate, 2008 A linkage map of the zebra finch Taeniopygia
796 guttata provides new insights into avian genome evolution. Genetics 179: 651–667.
797 Stapley J., P. G. D. Feulner, S. E. Johnston, A. W. Santure, and C. M. Smadja, 2017 Variation in
798 recombination frequency and distribution across eukaryotes: patterns and processes. Philos.
799 Trans. R. Soc. Lond. B Biol. Sci. 372: 20160455.
800 Stephens M., 2017 False discovery rates: a new deal. Biostatistics 18: 275–294.
801 Torgasheva A. A., and P. M. Borodin, 2017 Immunocytological Analysis of Meiotic Recombination in the
802 Gray Goose (Anser anser). Cytogenet. Genome Res. 151: 27–35.
803 Torgasheva A. A., L. P. Malinovskaya, K. S. Zadesenets, T. V. Karamysheva, E. A. Kizilova, *et al.*, 2019
804 Germline-restricted chromosome (GRC) is widespread among songbirds. Proc. Natl. Acad. Sci.
805 U. S. A. 116: 11845–11850.

Trivers R., 1988 Sex differences in rates of recombination and sexual selection, pp. 270–286 in *Evolution of Sex: An Examination of Current Ideas*, edited by Richard E. Michod B. R. L. Sinauer Associates Inc., Sunderland, Massachusetts.

VanRaden P. M., 2008 Efficient methods to compute genomic predictions. J. Dairy Sci. 91: 4414–4423.

Veller C., N. Kleckner, and M. A. Nowak, 2019 A rigorous measure of genome-wide genetic shuffling that takes into account crossover positions and Mendel's second law. Proc. Natl. Acad. Sci. U. S. A. 116: 1659–1668.

Warren W. C., D. F. Clayton, H. Ellegren, A. P. Arnold, L. W. Hillier, *et al.*, 2010 The genome of a songbird. Nature 464: 757–762.

Weng Z., A. Wolc, H. Su, R. L. Fernando, J. C. M. Dekkers, *et al.*, 2019 Identification of recombination hotspots and quantitative trait loci for recombination rate in layer chickens. J. Anim. Sci. Biotechnol. 10: 20.

Yang J., S. H. Lee, M. E. Goddard, and P. M. Visscher, 2011 GCTA: a tool for genome-wide complex trait analysis. Am. J. Hum. Genet. 88: 76–82.